



Cellular and molecular effects of protons: Apoptosis induction and potential implications for cancer therapy

C. Di Pietro*, S. Piro*, G. Tabbì, M. Ragusa, V. Di Pietro, V. Zimmitti, F. Cuda, M. Anello, U. Consoli, E. T. Salinaro, M. Caruso, C. Vancheri, N. Crimi, M. G. Sabini, G. A. P. Cirrone, L. Raffaele, G. Privitera, A. Pulvirenti, R. Giugno, A. Ferro, G. Cuttone, S. Lo Nigro, R. Purrello, F. Purrello† and M. Purrello

Dipartimento di Scienze Biomediche, Sezione di Biologia, Genetica e Bioinformatica, Università di Catania, 95123 Catania, Italy (C. Di Pietro, M. Ragusa, V. Di Pietro, V. Zimmitti, F. Cuda, A. Pulvirenti, R. Giugno, A. Ferro, M. Purrello); Dipartimento di Medicina Interna e Medicina Specialistica, Sezione di Endocrinologia, Università di Catania, Ospedale Garibaldi, 95124 Catania, Italy (S. Piro, M. Anello, F. Purrello); Istituto di Biostrutture e Bioimmagini, CNR, 95125 Catania, Italy (G. Tabbì); Dipartimento di Scienze Biomediche, Sezione di Ematologia, Università di Catania, 95124 Catania, Italy (U. Consoli); Dipartimento di Medicina Interna e Medicina Specialistica, Sezione di Malattie Respiratorie, Università di Catania, 95125 Catania, Italy (E. T. Salinaro, M. Caruso, C. Vancheri, N. Crimi); Istituto Nazionale di Fisica Nucleare, Laboratorio Nazionale del Sud, 95125 Catania, Italy (M. G. Sabini, G. A. P. Cirrone, L. Raffaele, G. Cuttone); Dipartimento di Diagnostica per Immagini e Radioterapia, Università di Catania, 95125 Catania, Italy (G. Privitera); Dipartimento di Matematica ed Informatica, Università di Catania, 95125 Catania, Italy (A. Pulvirenti, R. Giugno); Dipartimento di Fisica e di Astronomia, Università di Catania, 95125 Catania, Italy (S. Lo Nigro); Dipartimento di Scienze Chimiche, Università di Catania, 95125 Catania, Italy (R. Purrello)

Published online: 20 December 2005

Due to their ballistic precision, apoptosis induction by protons could be a strategy to specifically eliminate neoplastic cells. To characterize the cellular and molecular effects of these hadrons, we performed dose-response and time-course experiments by exposing different cell lines (PC3, Ca301D, MCF7) to increasing doses of protons and examining them with FACS, RT-PCR, and electron spin resonance (ESR). Irradiation with a dose of 10 Gy of a 26.7 MeV proton beam altered cell structures such as membranes, caused DNA double strand breaks, and significantly increased intracellular levels of hydroxyl ions, are active oxygen species (ROS). This modified the transcriptome of irradiated cells, activated the mitochondrial (intrinsic) pathway of apoptosis, and resulted in cycle arrest at the G2/M boundary. The number of necrotic cells within the irradiated cell population did not significantly increase with respect to the controls. The effects of irradiation with 20 Gy were qualitatively as well as quantitatively similar, but exposure to 40 Gy caused massive necrosis. Similar experiments with photons demonstrated that they induce apoptosis in a significantly lower number of cells and in a temporally delayed manner. These data advance our knowledge on the cellular and molecular effects of proton irradiation and could be useful for improving current hadrontherapy protocols.

Key words: apoptosis; cancer; cell cycle; FACS; hadrontherapy; proton beam; RT-PCR.

*Equal contribution

†Current address: Unità Operativa di Medicina Interna, Ospedale Cannizzaro, 95125 Catania, Italy

Correspondence to: M. Purrello, Dipartimento di Scienze Biomediche, Sezione di Biologia, Genetica e Bioinformatica, Università di Catania, 95123 Catania, Italy. Tel.: +39-95-3782078; Fax: +39-95-3782158; e-mail: purrello@unict.it

Introduction

Cell death may occur through different mechanisms: apoptosis, necrosis, autophagy, senescence, and mitotic catastrophe.¹ The pathways leading to apoptosis and necrosis are quite well known, whereas those of autophagy, senescence and mitotic catastrophe are still poorly characterized.¹ Apoptosis, the process responsible for the physiological elimination of cells during development, differentiation and at steady state, may be defined as a clean type of cell death. Contrary to necrotic cells, which are lysed with ensuing diffusion of inflammatory molecules, apoptotic cells activate pathways leading to their suicide and then undergo macrophage phagocytosis.²⁻⁵ The different phases of the apoptotic process (initiation, progression, and conclusion) are carried out by a complex apparatus, which has been well conserved during evolution⁶ (Purrello *et al.*, unpublished observations). Initiation is controlled by a set of proteins many of which belong to the *bcl-2* supergroup, even though they may have opposite functions: the *bcl-2* protein and members of its family are anti-apoptotic, whereas *bax-α* and related polypeptides are pro-apoptotic. The stoichiometric and functional equilibrium between the two groups determines the cell's fate.⁷⁻⁹ The apoptotic apparatus is functionally connected to other cell machineries, such as those controlling cell cycle and DNA duplication,¹⁰ cell proliferation and differentiation,^{11,12} genome stability,^{13,14} and cell metabolism.¹⁵⁻¹⁷ Accordingly, apoptosis may be considered an integral part of the biological program of all known organisms.¹⁸⁻²⁰ The increased knowledge of its molecular mechanisms²¹ could allow for the exploitation of apoptosis for innovative

approaches in cancer therapy. A general and effective strategy could entail the specific induction of suicide in neoplastic cells, while sparing healthy ones. One way to obtain this would be to expose solid tumors to appropriately low doses of highly focused ionizing radiations (IR), such as protons, with the objective of specifically inducing apoptosis in cancer cells. In this paper we report the results of a series of experiments aimed at characterizing the cellular and molecular effects of protons on different cell lines (PC3, Ca301D, MCF7), irradiated with increasing doses of protons and examined with FACS, RT-PCR, and electron spin resonance (ESR).

Materials and methods

Cell lines and culture conditions

PC3 and MCF7 cell lines derived from a bone metastasis of a prostate adenocarcinoma and from a mammary adenocarcinoma, respectively, were obtained from the American Tissue Type Culture Collection (Rockville, MD). Ca301D cells were isolated from a papillomatous carcinoma of the thyroid at the Sezione di Endocrinologia of the Dipartimento di Medicina Interna e Medicina Specialistica of the Università di Catania (Italy). Three days before irradiation, cell lines were plated in 25 cm² tissue culture flasks, which on the day of treatment were filled with medium and exposed to single doses of protons or photons ranging from 5 to 40 Gy. Each treated sample was matched with untreated controls.

Irradiation of cells with protons and photons

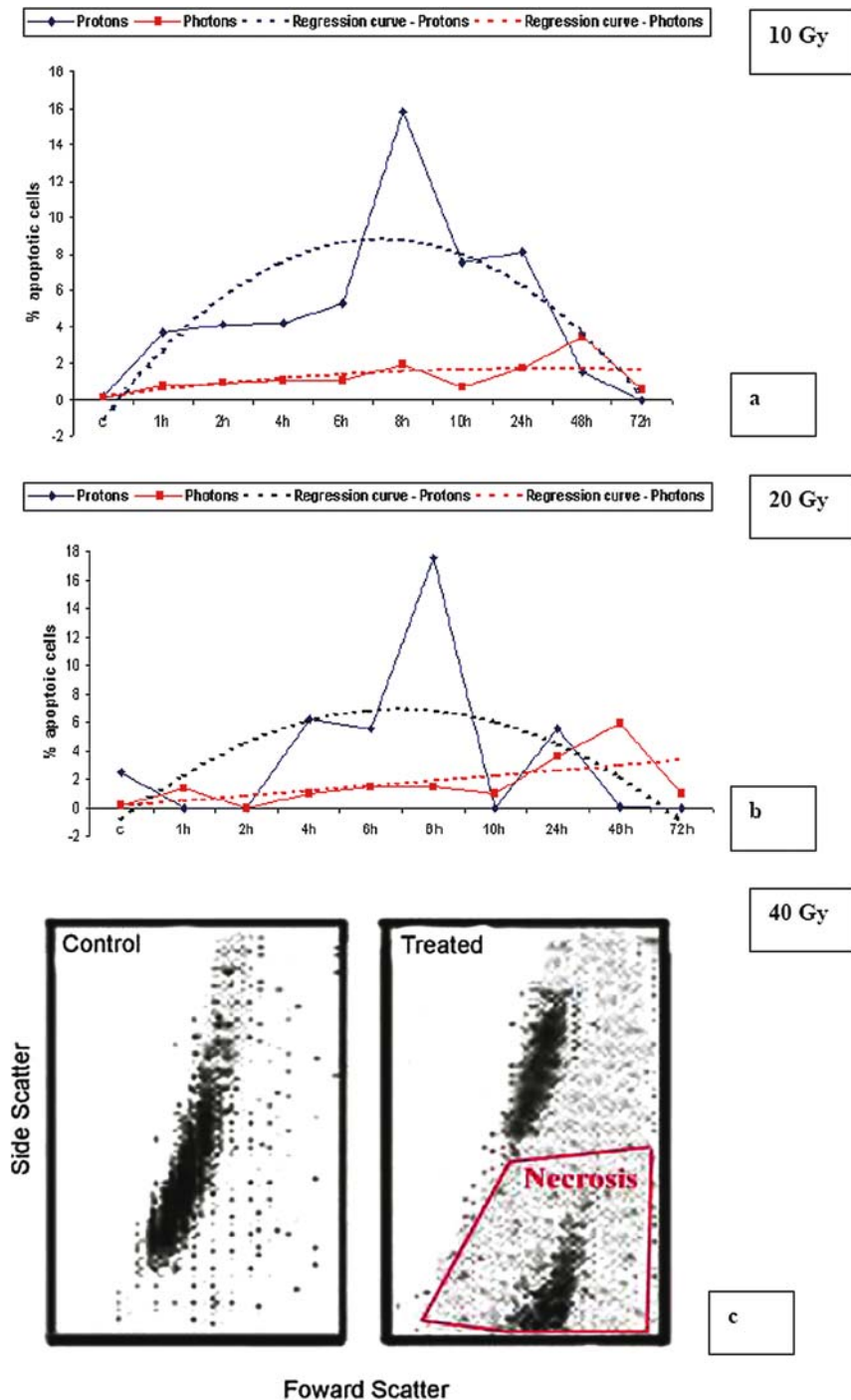
Proton irradiation was carried out at the Laboratori Nazionali del Sud (LNS) (Catania, Italy) of the Istituto Nazionale di Fisica Nucleare (INFN), using a Tandem Accelerator with a maximum accelerating voltage of 15 MV. In the experimental setup, a 26.7 MeV proton beam was delivered by the accelerator with a 190 μm thick gold scattering foil. The beam was extracted in air through the beamline exit window made of 75 μm thick aluminum. To match the shape of the tissue culture flasks, a collimator defining the boundaries of the irradiation field was mounted just in front of the target, which was suspended at 60 cm from the exit window. Dosimetry was carried out at 1 mm Perspex-equivalent depth, corresponding to the cell layer surface on the flask bottom. Accordingly, no dose correction had to be applied. The beam homogeneity was checked with radiographic films at different depths in PMMA phantom and found to be ±1%, as previously reported.²² Lateral uniformity of proton fluency at the target was almost 100%. Energy at the target was 22.6 MeV although there was some energy spread due to straggling.²³ Reference dosimetry was based on a parallel-plate Markus ionization chamber, calibrated with a high-energy electron beam according to the IAEA 381

protocol,²⁴ in comparison with a former cylindrical reference ionization chamber with a known cavity gas calibration factor. This had been determined in a secondary accredited calibration laboratory (PTW, Freiburg). The Markus chamber was compared with the reference ionization chambers of the Paul Scherrer Institute (Switzerland) and the Clatterbridge Center for Oncology (United Kingdom) in clinical proton dosimetry.²⁵ The same chamber was also used for depth dose measurements in a tissue equivalent medium. Given that the main radiobiological and clinical differences between X-rays and protons arise in the energy region below 30 MeV, where the RBE of protons is strongly increased, we concentrated our attention to this range. This was also based on the consideration that proton beams are completely stopped within the target, so that independently of the beam delivering system (active, spot scanning, passive scattering) a considerable quantity of protons with energy lower than 30 MeV will hit it. In most experiments the dose rate used was 1.46 Gy/min. After examining carefully that the corresponding biological effects were undistinguishable, in some experiments (*e.g.*, irradiation with 40 Gy) we used the dose rate of 7.3 Gy/min. Treatment with 5, 10, 20, and 40 Gy of 5 MeV photons was performed with a Linac ORION apparatus (General Electric) at the Dipartimento di Diagnostica per Immagini e Radioterapia (Università di Catania, Italy), according to standard procedures. Photons (2 Gy/min) were emitted from a source that was 100 cm from the flask. Irradiations were performed at isocenter (100 cm) with a field size of 10 × 10 cm and lateral uniformity of ±3%.

Cell population dynamics and detection of apoptosis or necrosis

At each time point after irradiation, irradiated cells and corresponding controls were collected (Figure 1a and b). To detect apoptosis or necrosis and to determine DNA content and the position of cells within the cell cycle, one aliquot was used for counting with standard microscopy methods, another for analysis with a FACS. Due to the inversion of cell membranes with externalization of phosphatidylserine, a phenomenon that is a well-known marker of apoptosis, Annexin V-FITC binds to it causing the apoptotic cell to emit fluorescence. Propidium Iodine enters necrotic cells, binds to their DNA and stains it. Cell fluorescence was assessed through a Flow Cytometer Coulter Epics Elite ESP (Coulter Corporation, Miami, FL, USA) by following standard procedures with an Annexin V-FITC Apoptosis Detection Kit (Sigma). Cells were gently scraped off the flasks, fixed by slow addition of absolute ethanol, left at -20°C for 16 h, centrifuged at 800 g for 10 min, washed once, resuspended with 500 μl of PBS containing RNase 100 ngr/ml, incubated for 1 h at 20°C, centrifuged at 800 g for 10 min, resuspended with 500 μl of PBS with BSA 1% and PI 50 μgr/ml, incubated for 15 min in the dark and examined with FACS. At least 10,000 forward side scatter gated events

Figure 1. Kinetics and extent of apoptosis induction in PC3 cells after irradiation with 10 Gy (panel a) and 20 Gy (panel b) of protons and photons, as determined through the annexin test and FACS analysis. Statistical analysis was performed by quadratic regression. Necrosis of PC3 and CA301D cells following exposure to 40 Gy of protons as determined through the annexin test and FACS analysis (panel c).



were collected per specimen. Identical procedures were performed on untreated controls. In many experiments, after incubation with annexin and PI, cells were also counted and analyzed with an inverted fluorescence microscope (Olympus IX 70), equipped with a dual filter set for FITC and rhodamine. The data obtained through either FACS or fluorescence microscope analysis were comparable. Cytoplas-

mic chromatin fragments, whose presence is another well known marker of apoptosis, were quantified with the Cell Death Detection ELISA Plus™ Kit (Roche Germany) according to the manufacturer's protocol. The amount of nucleosomes was determined photometrically by measuring the peroxidase retained in the immunocomplex. Cell viability and mitochondrial function were determined using

Table 1. RT-PCR primers

Gene	Accession number	Primers	cDNA (bp)	Forward start	Reverse start	PCR conditions
ATM	NM_000051	5'TGCTAACTGTGAGAAAGTTGC3' 5'AAAGACTCTGTTCCATTGAGG3'	407 bp	2071	2477	94°C 4 min; (94°C 60 sec, 51°C 90 sec, 72°C 120 sec)24x; 72°C 10 min;
p53	NM_000546	5'CCTGCCCTCAACAAGATGTTTTTG3' 5'TCAAAGCTGTTCCGTCCCAG3'	431 bp	633	1063	94°C 4 min; (94°C 60 sec, 60°C 90 sec, 72°C 120 sec)21x; 72°C 10 min;
p73	NM_005427	5'TGTCATCCCCTCCAACACC3' 5'TTCATGCCCCCTACACAGC3'	462 bp	449	62	94°C 4 min; (94°C 60 sec, 57°C 90 sec, 72°C 120 sec)30x; 72°C 10 min;
p63	NM_003722	5' GATGCTCTCTCTCCATCACC 3' 5'CCAGCACACTCTGTCTTCC 3'	394 bp	352	745	94°C 4 min; (94°C 60 sec, 54°C 90 sec, 72°C 120 sec)27x; 72°C 10 min;
p21	NM_000389	5'GGAACTTCGACTTTGTCACCGAG3' 5'GAACCTCTCATTCAACCGCCTAG3'	561 bp	240	800	94°C 4 min; (94°C 60 sec, 57°C 90 sec, 72°C 120 sec)25x; 72°C 10 min;
Bax	L22473	5'ACCAAGAAGCTGAGCGAGTGTC3' 5'ACAAAGATGGTCACGGTCTGCC3'	365 bp	166	530	94°C 4 min; (94°C 60 sec, 61°C 90 sec, 72°C 120 sec)27x; 72°C 10 min;
Bad	NM_032989	5'CCTTTAAGAAGGGACTTCCTCG3' 5'AAACCCAAAACCTCCGATGG3'	334 bp	371	704	94°C 4 min; (94°C 60 sec, 56°C 90 sec, 72°C 120 sec)25x; 72°C 10 min;
Bak	NM_001188	5'CACCAAGATTGCCACCAGC3' 5'CCTGCAAGGGAACAGAGAAGG3'	387 bp	533	919	94°C 4 min; (94°C 60 sec, 56°C 90 sec, 72°C 120 sec)25x; 72°C 10 min;
Bcl-2	M14745	5'CCACCAAGAAAGCAGGAAACC3' 5'ACAAAACCCACAGCAAAGG3'	400 bp	3118	3517	94°C 4 min; (94°C 60 sec, 59°C 90 sec, 72°C 120 sec)29x; 72°C 10 min;
Bcl-X _L	Z23115	5'GAATCACTAACCAGAGACG 3' 5' GGAAGAGTTCATTCACTACC 3'	476 bp	53	528	94°C 4 min; (94°C 60 sec, 49°C 90 sec, 72°C 120 sec)22x; 72°C 10 min;
SOD2	NM_000636	5'ACCACGATCGTTATGCTGAG3' 5'GGACTAGAAAGGCATCCCTACA3'	304 bp	674	977	94°C 4 min; (94°C 60 sec, 50°C 90 sec, 72°C 120 sec)25x; 72°C 10 min;
HPRT	NM_000194	5'CCTGCTGGATTACATTAAGCACTG3' 5'CTTCGTGGGGTCTTTTCACCAGC3'	282 bp	316	597	94°C 4 min; (94°C 60 sec, 60°C 90 sec, 72°C 120 sec)22x; 72°C 10 min;
β Actin	NM_001101	5'GCCAACCGTGAAAAGATGACC3' 5'TGCCGATAGTGATGACCTGACC3'	415 bp	340	754	94°C 4 min; (94°C 60 sec, 60°C 90 sec, 72°C 120 sec)18x; 72°C 10 min;

the 3-(4,5-dimethylthiazol-2-yl)-2,5-diphenyl tetrazolium bromide (MTT) assay that measures the cleavage of tetrazolium salts. Absorbance was measured at 545 nm using a 690 nm differential filter.

RT-PCR

RT-PCR analysis was performed as previously described.^{26–28} Primers for genes involved in apoptosis initiation, progression, conclusion, and in cell cycle control were designed with the program OMIGA (Oxford Molecular) using as template the cDNA segments shared by all known mRNA isoforms of the genes analyzed (Table 1). Total RNA was extracted with Trizol (Invitrogen)

from treated cells and untreated controls after scraping them off the flasks. This procedure was chosen to avoid damaging cell membranes with trypsin and the ensuing artifacts. Purity of RNA preparations and absence of contamination with DNA were confirmed by checking that the size of the amplified cDNAs was as expected and by performing PCR without the reverse transcription step. Reverse transcription of total RNA was performed for 1 h at 42°C using 1 μg of total RNA, 500 ng of oligo dT primers (Roche Molecular Biochemicals), and 200 U of Superscript II Reverse Transcriptase in a total volume of 20 μl of 1 × First Strand Buffer (Invitrogen). Different aliquots were amplified with 1U of Taq Platinum polymerase (Invitrogen) to determine the range of linearity between the amount of amplified cDNAs

and the mass of target mRNAs. Normalization was obtained by loading in the same gel well the cDNAs under study, together with control HPRT or β -actin cDNAs. These had been independently amplified from an identical aliquot of the same sample. Gel electrophoresis was performed in 1.5% agarose at 10 V/cm for 60 min. Gene specific cDNA quantification was repeated at least twice on each sample, with very similar results. Densitometric analysis was performed with an Image Master VDS using Total Lab software (Amersham Pharmacia Biotech, Little Chalfont, UK).

Electron spin resonance

ESR spectroscopic measurements were carried out as described on a Bruker ER 200 D spectrometer, driven by an ESP 3220 Data System and equipped with an NMR gaussmeter.²⁹ Spin trapping data were recorded at room temperature in a standard flat quartz cell. ESR spectra were simulated using the PEST Winsim program.³⁰ 5,5-Dimethyl-1-pyrroline N-oxide (DMPO) (Sigma) was used after vacuum distillation to remove orange paramagnetic impurities, which are present in commercial samples. The flasks containing the cell cultures (irradiated or controls) were emptied, cell layers were rinsed twice with 1 ml of unused culture medium; 1 ml of fresh medium, and 6.7 μ l of DMPO (final concentration 58 mM) were then added and left for 10 min at 20°C. Cells were scraped off and centrifuged at 800 g for 10 min at 4°C. The pellet was resuspended in 0.3 ml of medium and transferred to a flat quartz cell. To ascertain if reactive oxygen species (ROS) had been produced intracellularly, the cell pellet obtained from two 25 cm² flasks was resuspended in 0.4 ml of medium, homogenized manually by using a 0.5 ml glass homogenizer, and 2.7 μ l of DMPO were added to the resulting homogenate, which was examined by ESR. The minimal amount of ROS that could be detected in our assay was 0.05 μ M.

Statistical analysis

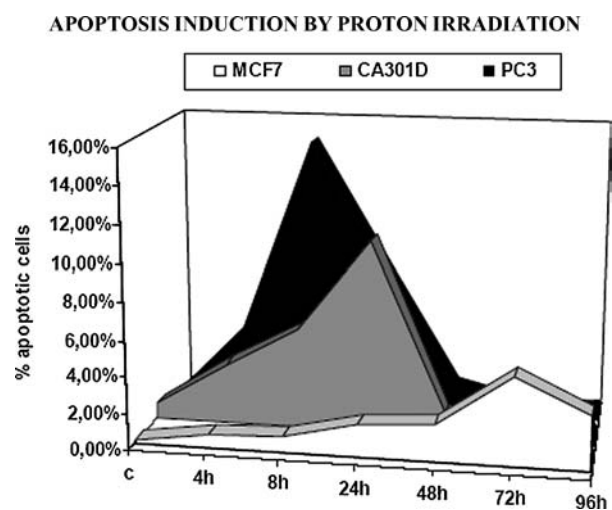
Statistical analysis was performed by quadratic regression of the set of points in the time series given by the degree of apoptosis and by the level of expression of key proteins of the apoptotic machinery.^{31,32} The regression parabolas approximate the general behaviour of the variables under analysis and allow a comprehensive global view of them.

Results

Proton induced apoptosis and cell cycle block

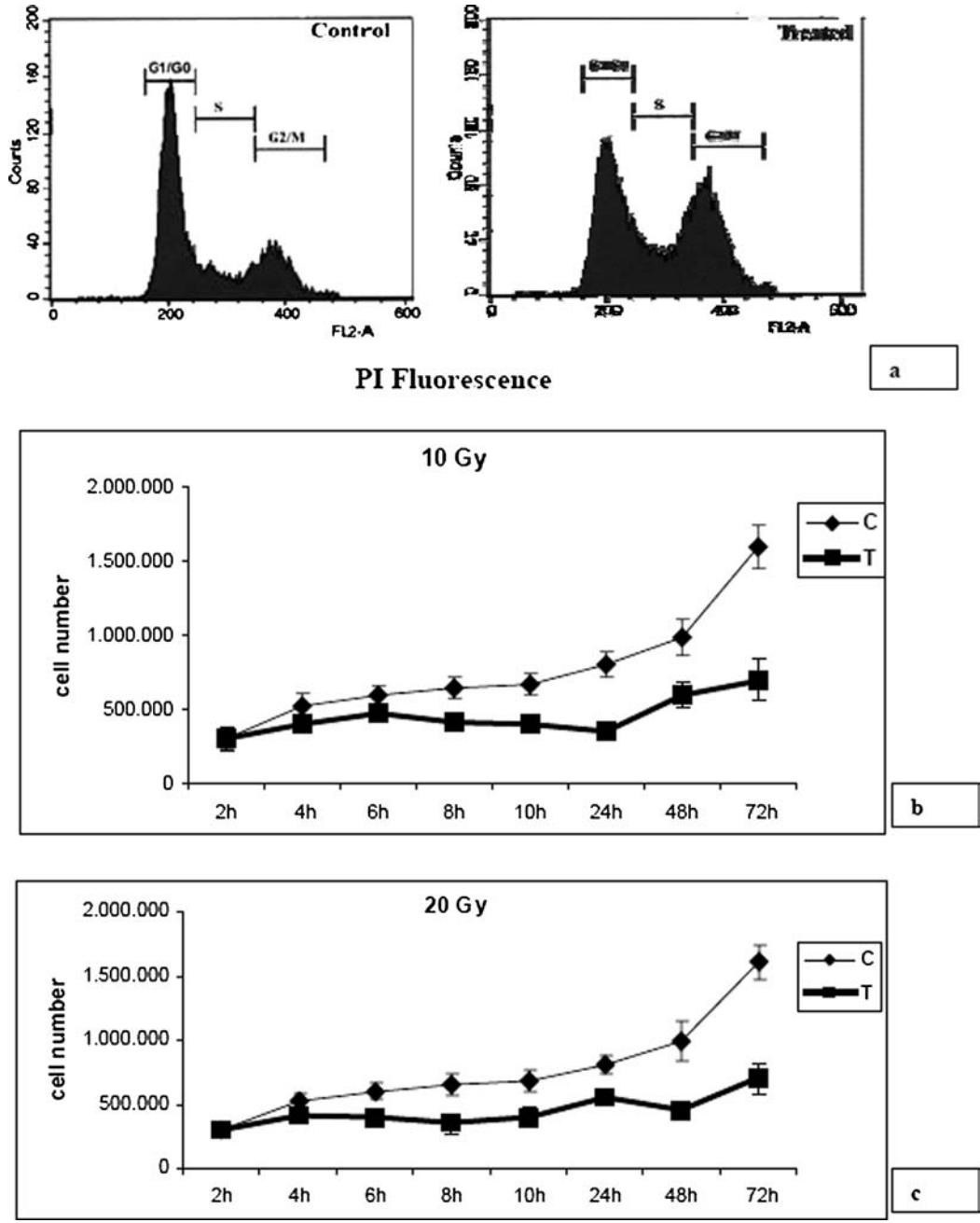
A dose-response study performed with Annexin V-FITC and FACS demonstrated that exposure to 5 Gy, 10 Gy, and 20 Gy of protons induced apoptosis in 6.1%, 15.8%, and 17.50% of PC3 cells, respectively (Figures 1a and b). Control cultures showed only background levels of

Figure 2. Kinetics and extent of apoptosis induction, as determined through the annexin test and FACS analysis, in PC3, Ca301D, and MCF7 cells treated with a 10 Gy proton beam. The graphs show the trend of values at the different time points chosen for the analysis.



apoptosis (>0.5%). The number of necrotic cells was similar in the two groups (0.5% \pm 0.2% and 0.6% \pm 0.4%, respectively). A dramatic change was seen after a single 40 Gy dose, which caused massive necrosis within 48 h of irradiation (Figure 1C). In CA301D cells 10 Gy of protons was the most effective dose as 10.5% of irradiated cells underwent apoptosis 24 h after irradiation (Figure 2). A time course-analysis demonstrated that after a single irradiation with 10 Gy of protons the percentage of apoptotic PC3 cells reached its peak 8 h after irradiation, whereas in CA301D cultures this occurred 24 h after treatment with the same dose of protons (Figure 2). Finally, 4.8% of MCF7 cells underwent apoptosis within 72 h following irradiation with 10 Gy of protons. The default value of apoptosis for the three cell lines didn't change significantly during the experiment (Figure 2). Also, the number of necrotic cells in CA301D and MCF7 cell lines remained at background levels after treatment. Cytoplasmic chromatin fragments were significantly increased in PC3 cells 8 h after irradiation with 10 Gy, in comparison to control cells (1.95 \pm 0.7 OD vs 0.42 \pm 0.1 OD, mean \pm ES; $n = 5$; $p > 0.001$). The number of metabolically active PC3 cells, as determined through the MTT assay, was significantly reduced after exposure to IR. This difference was present up to 48 h after treatment. Besides inducing apoptosis, irradiation with 10 Gy of protons also blocked PC3 cells at the G2/M interface (Figure 3a). This clearly altered the kinetics of the cell population growth, leading to a 2.3 fold cell number difference between control and treated samples 72 h after IR exposure (Figure 3b). A similar effect was caused by a dose of 20 Gy (Figure 3c). Exposure of CA301D cells to a 10 Gy proton beam also induced a cycle block at the G2/M interface, as already demonstrated for PC3 cells (not shown).

Figure 3. Panel a. FACS analysis of PC3 cells exposed to 10 Gy of protons, demonstrating their block at the G2/M phase of the cell cycle. Panels b and c. Kinetics of PC3 cell population growth after exposure to 10 and 20 Gy of protons. C: control samples; T: treated samples. $N = 5$; $p < 0.001$.



Effects of protons on the expression of mRNAs involved in the apoptotic process

Irradiation with 10 Gy of protons clearly altered the PC3, CA301D, and MCF7 mRNA phenotype at the different loci involved in apoptosis initiation, progression, conclusion, and cycle control. In PC3 cells 8 h after treatment when the number of cells with structural signs of apoptosis reached its peak (Figures 1a, 2), we detected a 2.1 fold increase of ATM mRNA, a 6.1 fold increase of p73 mRNA, and a 9.3

fold increase of p21 mRNA relative to controls (Figure 4a). At 10 h there was an 11 times increase of the Bcl-2/Bax- α ratio (Figure 4b). These changes were followed by an increase of SOD2 mRNA that reached its peak (three times higher than in controls) 24 h after irradiation (Figure 4a). There was no variation of the levels of mRNAs encoding Bad and Bak, two pro-apoptotic genes of the Bcl-2 family. Due to nonsense-mediated mRNA decay, no p53 mRNA may be detected in PC3 cells.^{33,34} When apoptosis of 10 Gy treated CA301D cells reached its maximum, 24 h after irradiation

Figure 4. mRNA phenotype variation in PC3 and in CA301D cells at the loci encoding ATM, p73, p21, and SOD2 after irradiation with a 10 Gy proton beam (panels a, c). Kinetics of the Bcl2/Bax- α ratio in PC3 cells (panel b) and of Bcl_{XL}/Bax α in CA301D cells (panel d).

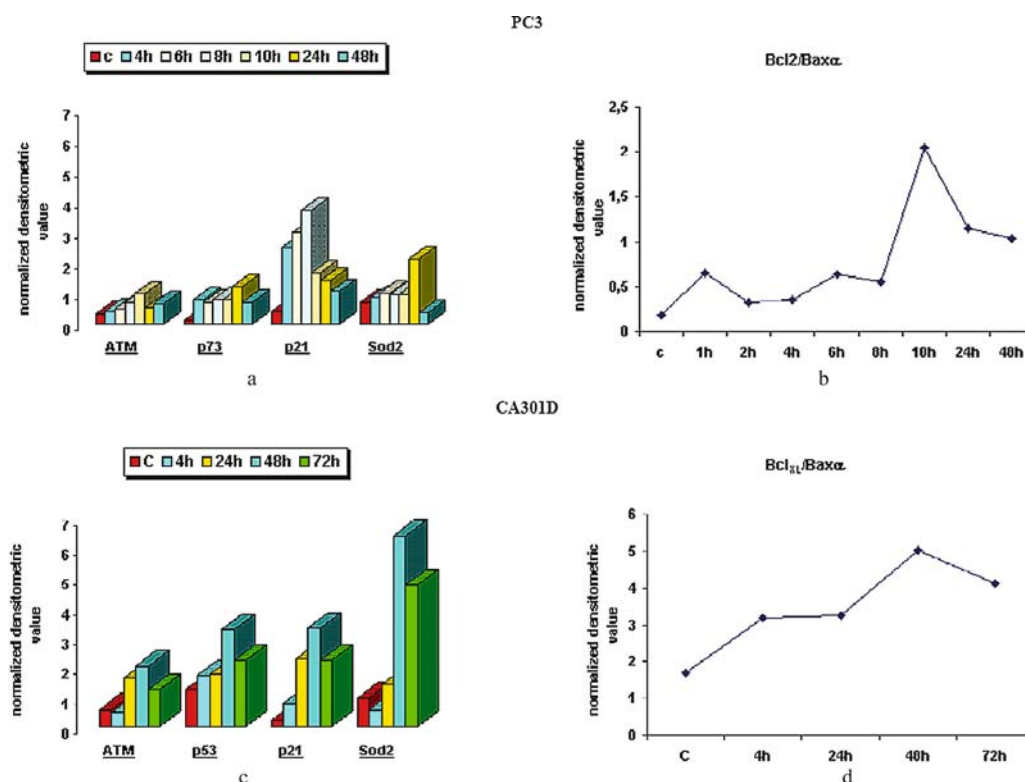


(Figure 2), the levels of the mRNAs encoding ATM, p53, and p21 were 2.8, 1.4, and 12 times higher than the controls (Figure 4c). At the disappearance of the morpho-structural signs of apoptosis, 48 h after irradiation, there was a 6.1 times increase of Bcl-X_L mRNA with a corresponding 2.9 times rise of its ratio over bax- α (Figure 4d). At the same time, SOD2 mRNA was 6.7 times more abundant in irradiated cells than in controls (Figure 4c). Due to nonsense-mediated mRNA decay, p73 mRNA is undetectable in CA301D cells (see above). In MCF7 cells, 72 h after treatment, the levels of Bcl-2 and Bax- α mRNAs were 2.5 and 7.8 times higher than the controls. 24 h later, Bcl-2 levels increased 1.95 times, and Bax- α levels increased 5 times, with their ratio becoming 2 from the previous value of 1.5 (data not shown).

Apoptosis induction by photons and corresponding variations of the transcriptome

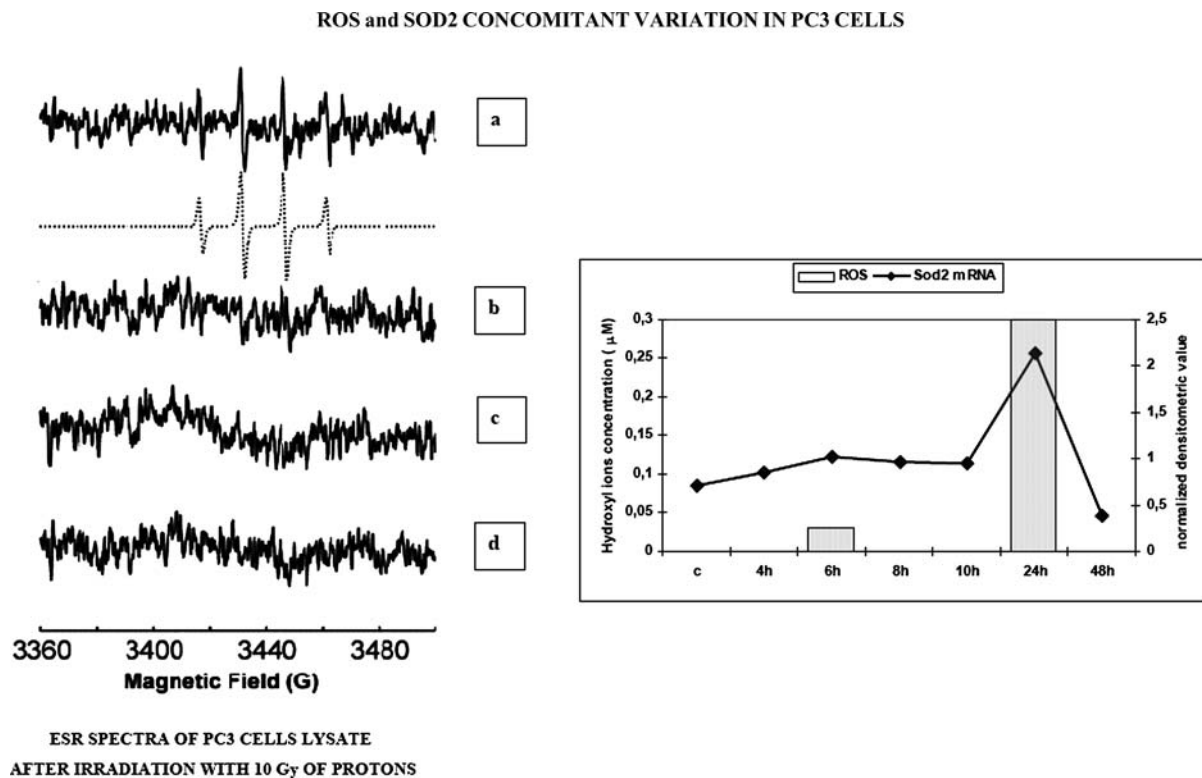
In contrast to protons, photons induced apoptosis in the PC3 cell line to a clearly lower extent and with an evident temporal delay at the doses of 10 and 20 Gy (Figures 1a-b). The peak of apoptosis, 3.5% and 6% of the treated cell population, was reached 48 h after irradiation with a single dose of either 10 or 20 Gy (Figure 1a-b). There was a 1.6 fold increase of Bax- α mRNA at 8 h after irradiation, together

with a 1.6 times increase of ATM mRNA followed by a 2.9 fold increase of Bcl-2 mRNA 2 h later. The Bcl-2/Bax- α ratio became 2.5 times higher than the controls 10 h after exposure to photons (data not shown). As already seen with protons, irradiation with 40 Gy of photons caused massive necrosis of treated cells (not shown).

Effects of protons on ROS intracellular concentration

To investigate whether irradiation with protons determined ROS production, we carried out spin trapping experiments. PC3 cells were exposed to 5, 10, and 20 Gy of protons and their ESR spectra were measured at 6 and 24 h after irradiation. Several spectra were recorded on samples irradiated with 10 Gy of protons. Measurements using whole cells showed that neither the cell suspension nor the medium had any trapped radical adduct, both at 6 and 24 h after irradiation (data not shown). Instead, the homogenate from cells analyzed 24 h after irradiation with 10 Gy clearly showed the hydroxyl radical adduct pattern, $a^N = 14.9$ G; $a^H = 14.9$ G, which was not detected in homogenized control cells nor in medium from irradiated and control cultures (Figure 5a-d). Based on an accurate calibration curve, we estimated that the concentration of hydroxyl ions

Figure 5. ESR spectra of samples, 24 h after irradiation, containing 58 mM DMPO and (a) homogenized irradiated PC3 cells; (b) homogenized control PC3 cells; (c) medium from irradiated PC3 cells; (d) medium from control PC3 cells. The pattern shown in (a) arises from the hyperfine coupling constant values, which a peculiar characteristics of the hydroxyl adduct with DMPO. The 1:2:2:1 ESR signal intensity of the quartet pattern comes from the perfect superimposition of two lines of two triplets due to the identity of the two hyperfine coupling constants a^H and a^N . The simulated spectrum (dotted line) was obtained using $a^H = 14.9$ G, $a^N = 14.9$ G. Instrument settings: modulation frequency, 100 kHz; modulation amplitude, 0.7 G; receiver gain 8×10^4 ; time constant, 81 ms; sweep rate, 285 G/min; microwave frequency, 9.77 GHz; microwave power, 40 mW, 30 scans. (e) Graph showing the relationship between the levels of hydroxyl ions and SOD2 mRNA.



was $0.3 \mu\text{M}$. No signal was found in the lysate from PC3 cells irradiated with 5 and 20 Gy and analyzed 24 and 6 h after treatment, respectively. Detection of hydroxyl radicals coincided with a significant increase of SOD2 mRNA levels (Figure 5e).

Discussion

Due to its incidence, fatalities, and the annual financial toll, it is generally agreed that cancer is the major medical problem of western societies.^{35,36} Distinct strategies have been designed for its treatment, such as surgery, radiotherapy,³⁷ chemotherapy,³⁸ and more recently, immunotherapy.^{39,40} It has been also suggested that exploitation of a biological phenomenon, such as apoptosis, could be an additional therapeutic strategy.^{41,42} This would be especially true if cell suicide could be induced by factors endowed with high target specificity. This specificity could be molecular by employing antibodies against tumor-specific antigens,³⁹ or spatial, if irradiation were performed with particles characterized by high ballistic precision such as protons, which produce little side scatter and stop abruptly at any prescribed depth

(Bragg peak), allowing the precise delivery of large doses of particles to irregular three-dimensional volumes.^{43,44} The data presented in this paper demonstrate that irradiation with 10 Gy of protons specifically induced apoptosis, but not necrosis, in a fraction of cells ranging from 15.8% (PC3) to 10.5% (CA301D) and 4.8% (MCF7). This was proven by the presence of different markers of cell suicide such as externalization of phosphatidylserine, release of chromatin fragments in the cytoplasm, and specific transcriptome modifications. The effects of irradiation with 20 Gy of protons were qualitatively as well as quantitatively similar to those of 10 Gy (Figures 1a and b), which suggests a plateau effect for these hadrons. We didn't observe a similar phenomenon with photons, at least within the dose range examined (Figures 1a and b). On the other hand, irradiation with 40 Gy of either protons or photons caused massive necrosis (Figure 1c). Proton irradiation also caused a block of PC3 and CA301D cell cycles at the G2/M interface. Our characterization of the mRNA phenotype of proton irradiated PC3, CA301D, MCF7 cells demonstrated induction of the cell cycle checkpoint ATM gene and of its downstream targets, such as p53 or members of its family (*e.g.*, p73), p21, and bax- α .^{45–48} The ensuing modifications of the cell phenotype

comprised alteration of mitochondrial functions and oxidative metabolism with overproduction of hydroxyl ions (a ROS) in PC3 cells, as well as damage to nucleic acids and membrane phospholipids.⁴⁹ The increase of SOD2 mRNA levels, shown in Figure 5, represents the reaction of cells to the deleterious effects of ROS on their structure.^{50–52} Our data clearly demonstrate the presence of hydroxyl ions in irradiated cells at a concentration of 0.3 μM with an estimated increase of sixty times over the minimum threshold level of 0.05 μM (see *Materials and Methods and Results*). The absence of hydroxyl radicals 24 h after irradiation with 5 Gy of protons suggests that their amount was below the threshold detection level. On the other hand, we hypothesize that the 6 h interval between treatment with 20 Gy and analysis was too short for the production of detectable amounts of ROS. Altogether, our results strongly suggest a major involvement of the mitochondrial (intrinsic) cell death pathway in the response to proton irradiation.^{2,52–54} These data significantly advance the existing knowledge on the biological effects of these hadrons. In fact, a previously published study examined cell viability after proton irradiation using only a clonogenic assay.⁵⁵ In another report on the effects of proton irradiation, activation of apoptosis in thyroid follicular cells was investigated by searching for different markers such as cytoplasmic DNA fragments and micronuclei.⁵⁶ These authors also reported a block of cell cycle at the G2 phase but didn't describe modifications of the mRNA phenotype nor the increase of ROS induced by proton irradiation.⁵⁶ It is interesting to note that also gamma irradiation of CCRF-CEM, a human lymphoblastic leukemia cell line, has been reported to induce arrest at the G2/M phase of the cycle.⁵⁷

Conclusions

When analyzed in the context of the existing literature, our data demonstrate that their specific phenotypes and genotypes are important for the response of cells to irradiation. In fact, the tendency of a cell to undergo cycle block and eventually apoptosis depends on its genotype and RNA and protein phenotype at the loci involved in cycle control, DNA repair, and apoptosis activation. Magnitude, kinetics, and specific sequence of events are expected to vary between different cell types (e.g., Figure 4a and 4c). Due to the well known variety of tumor genotypes and corresponding phenotypes,⁵⁸ this heterogeneity should be expected to be even more frequent in therapeutic settings. This clearly implies the need for treatment protocols designed for the specific tumor type or, even better, for the specific individual as required in the world of Molecular Medicine.⁵⁹ In this context, the characterization of the cellular and molecular response to proton irradiation of the most frequent tumour types will be useful to allow for a rational design of treatment protocols. The worldwide increase of the number of cancer patients treated with hadrontherapy as well as of the number of hadronther-

apy centers under construction⁶⁰ warrant further studies to elucidate the cellular and molecular effects of proton irradiation and the underlying mechanisms.

Acknowledgments

We thank Prof R Vigneri for the generous gift of cell line CA301D, Prof R Giustolisi for kindly allowing us to perform some of the experiments with the FACS instrument at the Sezione di Ematologia, Dipartimento di Scienze Biomediche, Università di Catania. We also thank Drs D Barbagallo, M Caruso, F Frasca, P Lo Iacona, E Modica, G Pandini, V Patti, D Spampinato, A Valastro, and Mr R Russo for their kind collaboration. Finally, we thank Dr G Scacciante (Amersham Pharmacia) for his very kind help. This project was supported by funds from MIUR (Ministero dell'Istruzione, dell'Università e della Ricerca), Piani di Potenziamento della Rete Scientifica e Tecnologica. These data were presented as an oral presentation at the 5th International Symposium on Swift Heavy Ions in Matter, Taormina (Italy), May 22–25, 2002 and at the International Symposium on Impact of Biotechnology on Predictive Oncology and Intervention Strategies, Nice (France), February 7–10, 2004.

References

- Okada H, Mak TW. Pathways of apoptotic and non-apoptotic death in tumour cells. *Nature Rev Cancer* 2004; 4: 592–603.
- Kerr JFR, Harman BV. Definition and incidence of apoptosis. In: Tomei LD, Cope FO, eds. *Apoptosis, the Molecular Bases of Cell Death*, Cold Spring Harbor Laboratory Press 1991: 5–29.
- Hengartner MO. The biochemistry of apoptosis. *Nature* 2000; 407: 770–776.
- Meier P, Finch A, Evan G. Apoptosis in development. *Nature* 2000; 407: 796–801.
- Savill J, Fadok V. Corpse cleaning defines the meaning of cell death. *Nature* 2000; 407: 784–788.
- Aravind L, Dixit VM, Koonin EV. Apoptotic molecular machinery: Vastly increased complexity in vertebrates revealed by genome comparisons. *Science* 2001; 291: 1279–1284.
- Adams JM, Cory S. The Bcl-2 protein family: Arbiters of cell survival. *Science* 1998; 281: 1322–1326.
- Korsmeyer SJ. Bcl-2 gene family and the regulation of programmed cell death. *Cancer Res* 1999; 59: 1693s–1700s.
- Cory S, Adams JM. The Bcl-2 family: Regulators of the cellular life-or-death switch. *Nature Rev Cancer* 2002; 2: 647–656.
- Murray AW, Marks D. Can sequencing shed light on cell cycling? *Nature* 2001; 409: 844–846.
- Evan G, Littlewood TA. A matter of life and death. *Science* 1998; 281: 1317–1321.
- Evan GI, Vousden KH. Proliferation, cell cycle and apoptosis in cancer. *Nature* 2001; 411: 342–348.
- Hoeijmakers JH. Genome maintenance mechanisms for preventing cancer. *Nature* 2000; 411: 366–374.
- Wood RD, Mitchell M, Sgouros J, Lindahl T. Human DNA repair genes. *Science* 2001; 291: 1284–1289.

15. Saraste M. Oxidative phosphorylation at the *fin de siècle*. *Science* 1999; 283: 1488–1492.
16. Martinou JC, Green DR. Breaking the mitochondrial barrier. *Nature Rev* 2001; 283: 63–67.
17. Zamzani N, Kroemer G. The mitochondrion in apoptosis. *Nature Rev* 2001; 2: 67–71.
18. Michaelson J. The significance of cell death. In: Tomei LD and Cope FO, eds. *Apoptosis, the Molecular Bases of Cell Death*. Cold Spring Harbor Laboratory Press 1991: 31–46.
19. Lockshin RA, Zakeri Z. Programmed cell death and apoptosis. In: Tomei LD, Cope FO, eds. *Apoptosis, the Molecular Bases of Cell Death*. Cold Spring Harbor Laboratory Press 1991: 47–60.
20. Koonin EV, Aravind L. Origin and evolution of eukaryotic apoptosis: The bacterial connection. *Cell Death Diff* 2002; 9: 394–404.
21. Proceedings of the Meeting *Apoptosis: From signaling pathways to therapeutic tools*. <http://www.transduction-meeting.lu> 2003.
22. Onori S, De Angelis C, Fattibene P, et al. Dosimetric characterization of silicon and diamond detectors in low energy proton beams. *Phys Med Biol* 2000; 45: 3045–3058.
23. Raffaele L, Cuttone G, Barone Tonghi L. Use of 70 MeV proton beam for medical application at INFN—LNS. Proceedings of the International Conference on Nuclear Data, ISFN, Trieste, 1997; 1668–1673.
24. IAEA, Technical Reports Series, IAEA, Vienna 1997: 381.
25. Cuttone G, Raffaele L, Barone Tonghi L. First dosimetry intercomparison results for the CATANA Project. *Phys Med* 1999; 15: 121–130.
26. Purrello M, Scalia M, Corsaro C, Di Pietro C, Piro S, Sichel G. Melanosynthesis, differentiation and apoptosis in Kupffer cells from *Rana esculenta*. *Pigment Cell Res* 2001; 14: 126–131.
27. Purrello M, Di Pietro C, Rapisarda A, et al. Genes for human general transcription initiation factors TFIIB, TFIIB-Associated Proteins, TFIIC2, and PTF/SNAPC: Functional and positional candidates for tumour predisposition or inherited genetic diseases? *Oncogene* 2001; 20: 4877–4883.
28. Piro S, Patanè G, Di Pietro C, et al. Exposure to FFA or to high levels of glucose increases apoptosis in rat pancreatic islets cells. *Metabolism* 2002; 51: 1340–1347.
29. Tabbi G, Fry SC, Bonomo RP. ESR study of non-enzymic scission of xyloglucan by an ascorbate—H₂O₂-copper system: The involvement of the hydroxyl radical and the degradation of ascorbate. *J Inorg Biochem* 2001; 84: 179–187.
30. Duling DR. Simulation of multiple isotropic spin trap EPR spectra. *J Magn Res* 1994; 104: 105–110.
31. Cramer H. *Mathematical Methods of Statistics*. Princeton University Press, Princeton, USA 1946.
32. Dudewicz EJ, Mishra SN. *Modern Mathematical Statistics*, Wiley New York, USA 1988.
33. Hamid T, Kakar SS. PTTG/securin activates expression of p53 and modulates its function. *Mol Cancer* 2004; 3: 18.
34. Neu-Yilik G, Gehring NH, Hentze MW, Kulozik AE. Nonsense-mediated mRNA decay: From vacuum cleaner to Swiss army knife. *Genome Biol* 2004; 5: 218.
35. Peto J. Cancer epidemiology in the last century and the next decade. *Nature* 2001; 411: 390–395.
36. American Cancer Society. Cancer Facts and Figures <http://www.cancer.org>. 2002.
37. Lewanski CR, Gullick WJ. Radiotherapy and cellular signalling. *The Lancet Oncol* 2001; 2: 366–370.
38. Johnstone RW, Ruefli AA, Lowe SW. Apoptosis: A link between cancer genetics and chemotherapy. *Cell* 2002; 108: 153–164.
39. Rosenberg SA. Progress in human tumour immunology and immunotherapy. *Nature* 2000; 411: 380–384.
40. Appelbaum FR. Haematopoietic cell transplantation as immunotherapy. *Nature* 2000; 411: 385–389.
41. Nicholson DW. From bench to clinic with apoptosis based therapeutic agents. *Nature* 2000; 407: 810–816.
42. Tamm I, Schriever F, Dorken B. Apoptosis: Implications of basic research for clinical oncology. *The Lancet Oncol*. 2001; 2: 33–42.
43. Hug FB, Nevinny-Stickel M, Fuss M, Miller DW, Shaefer RA, Slater JD. Conformal proton radiation treatment for retroperitoneal neuroblastoma: Introduction of a novel technique. *Med Ped Oncol* 2001; 37: 36–41.
44. Noel G, Habrand JL, Helfre S, et al. Proton beam therapy in the management of central nervous system tumors in childhood: The preliminary experience of the Centre de Protontherapie d'Orsay. *Med Ped Oncol* 2003; 40: 309–315.
45. Polyak K, Xia Y, Zweier JL, Kinzler KW, Vogelstein B. A model for p53 induced apoptosis. *Nature* 1997; 389: 300–306.
46. Carr AM. Piecing together the p53 puzzle. *Science* 2000; 287: 1765–1766.
47. Flores ER, Tsai KY, Crowley D, et al. p63 and p73 are required for p53—dependent apoptosis in response to DNA damage. *Nature* 2000; 416: 560–564.
48. Vogelstein B, Lane D, Levine AJ. Surfing the p53 network. *Nature* 2000; 408: 307–310.
49. Khan AUK, Wilson T. Reactive oxygen species as cellular messengers. *Curr Biol* 1995; 2: 437–445.
50. Motoori S, Majima HJ, Ebara M, et al. Overexpression of mitochondrial Manganese Superoxide Dismutase protects against radiation induced cell death in the human hepatocellular carcinoma cell line HLE. *Cancer Res* 2001; 61: 5382–5388.
51. Epperly MW, Sikora CA, De Filippi SJ, et al. Manganese superoxide dismutase (SOD2) inhibits radiation induced apoptosis by stabilization of the mitochondrial membrane. *Rad Res* 2002; 157: 568–577.
52. Kroemer G, Zamzami N, Susin SA. Mitochondrial control of apoptosis. *Immun Today* 1997; 18: 44–51.
53. Rich T, Allen RL, Wyllie AH. Defying death after DNA damage. *Nature* 2000; 407: 777–781.
54. Li L, Story M, Legerski RJ. Cellular responses to ionizing radiation damage. *Int J Rad Oncol Biol Phys* 2001; 49: 1157–1162.
55. Belli M, Bettega D, Calzolari P, et al. Inactivation of human normal and tumour cells irradiated with low energy protons. *Int J Radiat Biol* 2000; 76: 831–839.
56. Green LM, Murray DK, Tran DT, et al. Response of thyroid follicular cells to gamma irradiation compared to proton irradiation. I. Initial characterization of DNA damage, micronucleus formation, apoptosis, cell survival, and cell cycle phase redistribution. *Radiat Res* 2001; 155: 32–42.
57. Strasser-Wozak EMC, Hartmann BL, Geley S, et al. Irradiation induces G2/M cell cycle arrest and apoptosis in p53-deficient lymphoblastic leukaemia cells without affecting Bcl-2 and Bax expression. *Cell Death Diff* 1998; 5: 687–693.
58. Ponder BA. Cancer Genet. *Nature* 2001; 411: 336–341.
59. Tate SK, Goldstein DB. Will tomorrow's medicines work for everyone? *Nature Genet* 2004; 36: 34–42.
60. Amaldi U. Future trends in cancer therapy with particle accelerators. *Z Med Phys* 2004; 14: 7–16.